Electronic Supplementary Material (ESI) for Physical Chemistry Chemical Physics.
This journal is © the Owner Societies 2016

SUPPLEMENTARY INFORMATION

ANALYSIS OF RAMAN SPECTRA

Figure 2 in the main text includes the Raman spectra, which provides information about the structural organization of the free carbon phase in PDCs. The representative features of free carbon in Raman spectra are the so called disorder induced D band at approximately 1350 cm^{-1} and the G band at approximately 1580 cm^{-1} due to in-plane bond stretching of sp^2 carbon.

Figure 2a shows that up to 1023 K the Raman spectra of the TTCS derived powders exhibit no significant feature due to a completely amorphous carbon phase,[79] while in the Raman spectrum obtained after pyrolysing up to 1273 K both the D and G bands appear due to the formation of free carbon nanocrystalline clusters and G´-band, [74-78]. Figure 2b includes the Raman spectra of the residues obtained of the pyrolysed CERASET precursor. In these residues, no significant features are noticed even at 1273 K, with only a very broad band due to a completely amorphous carbon phase. The lack of features of the Raman spectra obtained of the Ceraset derived SiCN ceramic might be striking at first since that composition usually exhibits well defined D and G bands at that temperature. However, it should noted that samples reported in literature are mostly prepared by heating the crosslinked precursor in a furnace up to 900-1000ºC for at least 1 or 2 hours in order to complete the ceramification process. In our case, we have measured the Raman spectra on powder samples retrieved directly from the TGA instrument after heating at a given temperature (550, 750 and 1000ºC) and then quenched to stop the reaction. This shows that just reaching 1000 ºC is not enough to fully develop the nanocrystalline structure of the free carbon in the ceramic but keeping the temperature for a minimum time might be necessary.

We have used the same Ceraset precursor to fabricate cylindrical pellets using more conventional procedures (heating up to 1000 to 1400 ºC and keeping the temperatures for 2 hours in a conventional furnace). In those cases we obtained the usual Raman spectra observed in these compositions, as shown in the figure below:

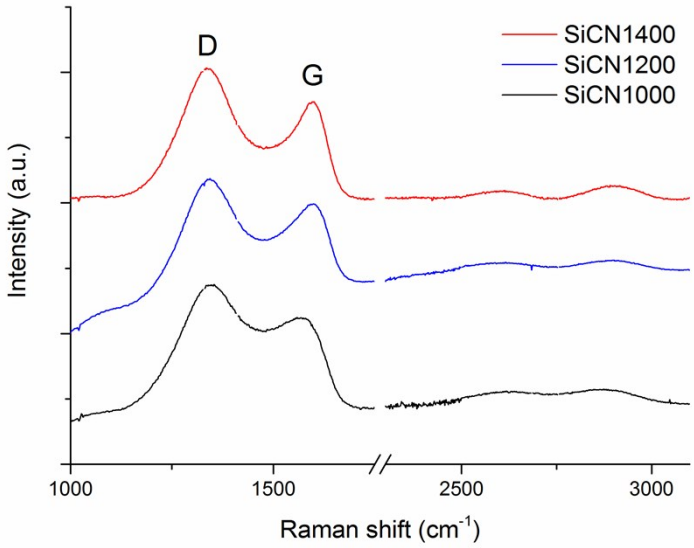

However, SiCO ceramics display reasonably well-defined D and G peaks after the same experimental procedure. This different behavior might be explained in terms of free carbon content, which is slightly under 20% in SiCN and about 35% in SiCO. It would be reasonable to assume that the formation of the nanocrystalline carbon domains large enough to be observed by Raman would be favoured in a composition with a higher carbon content.

ANALYSIS OF FTIR SPECTRA

Figure 3**a** in the main text shows the FTIR spectra of the cross-linked TTCS polymer and the subsequent powders obtained at 823 K, 1023 K and 1273 K. The figure shows the gradual transformation of the initial polymeric network into the final SiCO ceramic. Initially, the polymer network features bands at ~800-900 cm^{-1} are observed due to vibrations of Si-H bonds,[80] as well as bands at 2880 cm^{-1} and 1140 cm^{-1}, which are related to ethylene groups[80]. Such bands decrease in intensity with the temperature as the organic groups are cleaved and released, and are completely absent in the powder obtained at 1023 K. The bands at 2960, 1406 and 1260 cm^{-1} are produced by CH_3 groups[80] and also decrease with the pyrolysis temperature. The rearrangements of the bands at 1030 cm^{-1} due to Si-O bond asymmetric stretching vibrations[80] can be observed. The spectrum of the final SiCO ceramic shows only broad bands at 1031, 823 and 452 cm^{-1} corresponding to of Si-O and Si-C bonds vibrations. Figure 3b includes the FTIR spectra of the cross-linked CERASET polymer and the powders pyrolysed at 823 K, 1023 K and 1273 K. The spectra recorded for the powders collected at 823K presents features bands that can be attributed to N-H (3383 cm^{-1}), Si-H (2129 cm^{-1}), Si-N (794 and 898 cm^{-1}), C-H (2900, 2957 and 3048 cm^{-1}), $CH{=}CH_2$ (1593 cm^{-1}) and Si-CH_3 (1255 cm^{-1}). At 1023 K most of the aforementioned bands are absent and only appear broad bands at 750-1200 cm^{-1}, 2129 cm^{-1} and 3000-3400 cm^{-1}, attributed to Si-N, Si-H and N-H respectively[81]. At 1273 K only the broad Si-N band is noticeable.

KINETIC ANALYSIS – DECONVOLUTION OF EXPERIMENTAL COMPLEX CURVES

Table S1. Fitting parameters (a_0, a_1, a_2 y a_3) obtained by Fraser-Suzuki deconvolution of the experimental kinetic curve obtained for the thermal decomposition of TTCS precursor curves using Peakfit software.

THERMAL DECOMPOSITION TTCS PRECURSOR

	PROCESS 1					
	a_0	**a_1**	**a_2**	**a_3**	**Area**	**r^2**
2 K/min	0.00025	759	66	-0.10	55.41	0.998
5 K/min	0.00061	775	70	-0.10	43.10	0.997
7.5 K/min	0.00091	789	69	-0.04	59.73	0.998
10 K/min	0.00124	791	69	-0.01	61.88	0.998
	PROCESS 2					
	a_0	**a_1**	**a_2**	**a_3**	**Area**	**r^2**
2 K/min	0.000115	820	85	-0.05	33.14	0.998
5 K/min	0.000255	838	85	-0.03	40.85	0.997
7.5 K/min	0.00035585	854	85	-0.08	28.81	0.998
10 K/min	0.00045245	858	82	-2.345E-09	26.94	0.998
	PROCESS 3					
	a_0	**a_1**	**a_2**	**a_3**	**Area**	**r^2**
2 K/min	4.0833E-05	979	105	-0.6	11.45	0.998
5 K/min	0.000098	999	110	-0.6	16.05	0.997
7.5 K/min	0.00013869	1015	110	-0.6	11.46	0.998
10 K/min	0.000177	1027	115	-0.55	11.18	0.998

Table S2. Fitting parameters (a_0, a_1, a_2 y a_3) obtained by Fraser-Suzuki deconvolution of the experimental kinetic curve obtained for the thermal decomposition of CERASET precursor curves using peakfit software.

THERMAL DECOMPOSITION CERASET PRECURSOR

	PROCESS 1					
	a_0	**a_1**	**a_2**	**a_3**	**Area**	**r^2**
1 K/min	0.000057	707	89	-0.09	30.57	0.991
2 K/min	0.000098	727	92	-0.09	27.82	0.996
5 K/min	0.000246	755	92	-0.09	28.30	0.997
10 K/min	0.000490	767	90	-0.09	27.72	0.994
	PROCESS 2					
	a_0	**a_1**	**a_2**	**a_3**	**Area**	**r^2**
1 K/min	0.000022	784	70	-0.06	9.33	0.991
2 K/min	0.000034	807	70	-0.01	7.32	0.996
5 K/min	0.000085	835	70	-0.06	7.46	0.997
10 K/min	0.000175	856	80	-0.06	8.79	0.994
	PROCESS 3					
	a_0	**a_1**	**a_2**	**a_3**	**Area**	**r^2**
1 K/min	0.000063	864	110	-0.01	41.93	0.991
2 K/min	0.000130	878	110	-0.01	43.99	0.996
5 K/min	0.000312	903	110	-0.01	42.95	0.997
10 K/min	0.000596	922	120	-0.01	44.82	0.994
	PROCESS 4					
	a_0	**a_1**	**a_2**	**a_3**	**Area**	**r^2**

1 K/min	0.000034	943	90	-0.06	18.17	0.991
2 K/min	0.000068	972	100	-0.06	20.87	0.996
5 K/min	0.000170	1000	100	-0.06	21.29	0.997
10 K/min	0.000297	1023	100	-0.06	18.67	0.994

FIGURES

Fig. S1 Powders obtained during the ceramification TTCS precursor at 823, 1023 and 1273 K and initial cross-linked precursor. The evolution of colour is observed in figure.

Fig. S2 a) XRD spectra obtained for all the initial cross-linked TTCS precursor and the powders collected after interrupting the pyrolysis at 823, 1023, 1273 K. **b)** XRD spectra obtained for all the initial cross-linked CERASET precursor and the powders collected after interrupting the pyrolysis at 823, 1023, 1273 K.

Fig. S3. a) SEM images of the TTCS cross-linked precursor before ceramification and **b)** TTCS pyrolysed powder obtained at 1273K. **c)** SEM images of the CERASET cross-linked precursor before ceramification and **d)** CERASET pyrolysed powder obtained at 1273K.

Fig. S4 Experimental Kinetic curves (dα/dt-T and signals m/z) obtained for the thermal decomposition of TTCS under Ar gas flow and linear heating rate 2 K $min^{-1}$and registered flow gas in spectrometer mass during the thermal decomposition

Fig. S5 Experimental Kinetic curves (dα/dt-T and signals m/z) obtained for the thermal decomposition of TTCS under Ar gas flow and linear heating rate 7.5 K $min^{-1}$and registered flow gas in spectrometer mass during the thermal decomposition

Fig. S6a Experimental kinetic curve (symbols) obtained for the thermal decomposition of TTCS at linear heating rate 2 K min^{-1} and the Fraser-Suzuki function (solid line) used for fitting the simulated curves. Three independent stages are plotted with dotted lines. Correlation coefficient has been included into the figure.

Fig. S6b. Experimental kinetic curve (symbols) obtained for the thermal decomposition of TTCS at linear heating rate 7.5 K min^{-1} and the Fraser-Suzuki function (solid line) used for fitting the simulated curves. Three independent stages are plotted with dotted lines. Correlation coefficient has been included into the figure.

Fig. S6c. Experimental kinetic curve (symbols) obtained for the thermal decomposition of TTCS at linear heating rate 10 K min^{-1} and the Fraser-Suzuki function (solid line) used for fitting the simulated curves. Three independent stages are plotted with dotted lines. Correlation coefficient has been included into the figure.

Fig. S7. Experimental Kinetic curves (dα/dt-T and signals m/z) obtained for the thermal decomposition of CERASET under Ar gas flow and linear heating rate 2 K $min^{-1}$and registered flow gas in spectrometer mass during the thermal decomposition.

Fig. S8. Experimental Kinetic curves (dα/dt-T and signals m/z) obtained for the thermal decomposition of CERASET under Ar gas flow and linear heating rate 10 K $min^{-1}$and registered flow gas in spectrometer mass during the thermal decomposition.

Fig. S9a. Experimental kinetic curve (symbols) obtained for the thermal decomposition of CERASET at linear heating rate 1 K min^{-1} and the Fraser-Suzuki function (solid line) used for fitting the simulated curves. Four independent stages are plotted with dotted lines. Correlation coefficient has been included into the figure.

Fig. S9b. Experimental kinetic curve (symbols) obtained for the thermal decomposition of CERASET at linear heating rate 2 K min^{-1} and the Fraser-Suzuki function (solid line) used for fitting the simulated curves. Four independent stages are plotted with dotted lines. Correlation coefficient has been included into the figure.

Fig. S9c. Experimental kinetic curve (symbols) obtained for the thermal decomposition of CERASET at linear heating rate 10 K min^{-1} and the Fraser-Suzuki function (solid line) used for fitting the simulated curves. Four independent stages are plotted with dotted lines. Correlation coefficient has been included into the figure.

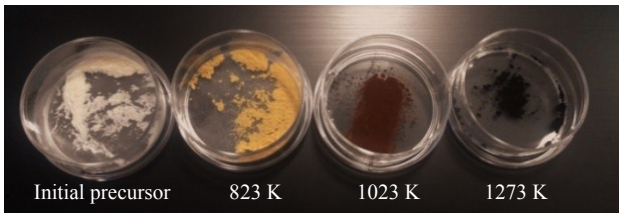

Fig. S1 Powders obtained during the ceramification TTCS precursor at 823, 1023 and 1273 K and initial cross-linked precursor. The evolution of colour is observed in figure.

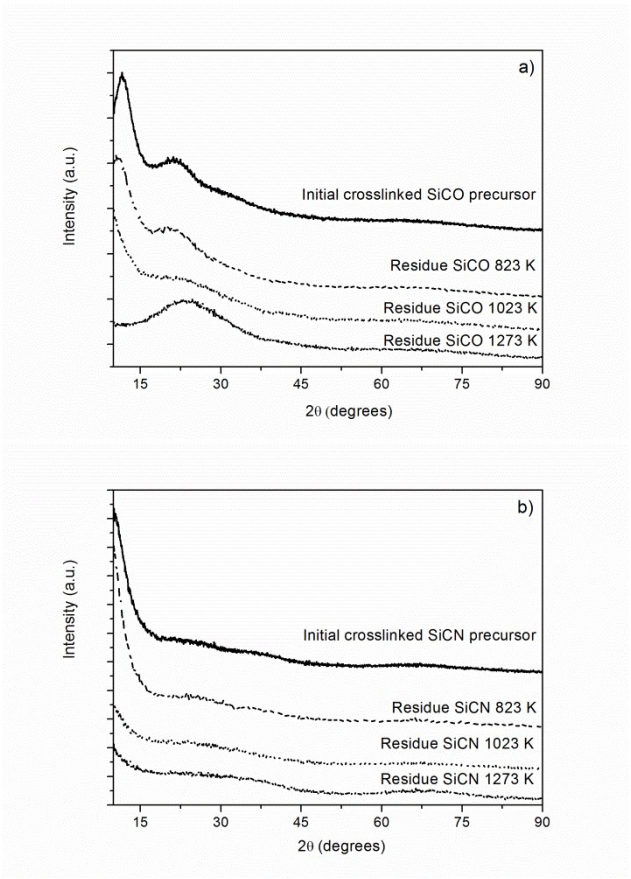

Fig. S2 a) XRD spectra obtained for all the initial cross-linked TTCS precursor and the powders collected after interrupting the pyrolysis at 823, 1023, 1273 K. **b)** XRD spectra obtained for all the initial cross-linked CERASET precursor and the powders collected after interrupting the pyrolysis at 823, 1023, 1273 K.

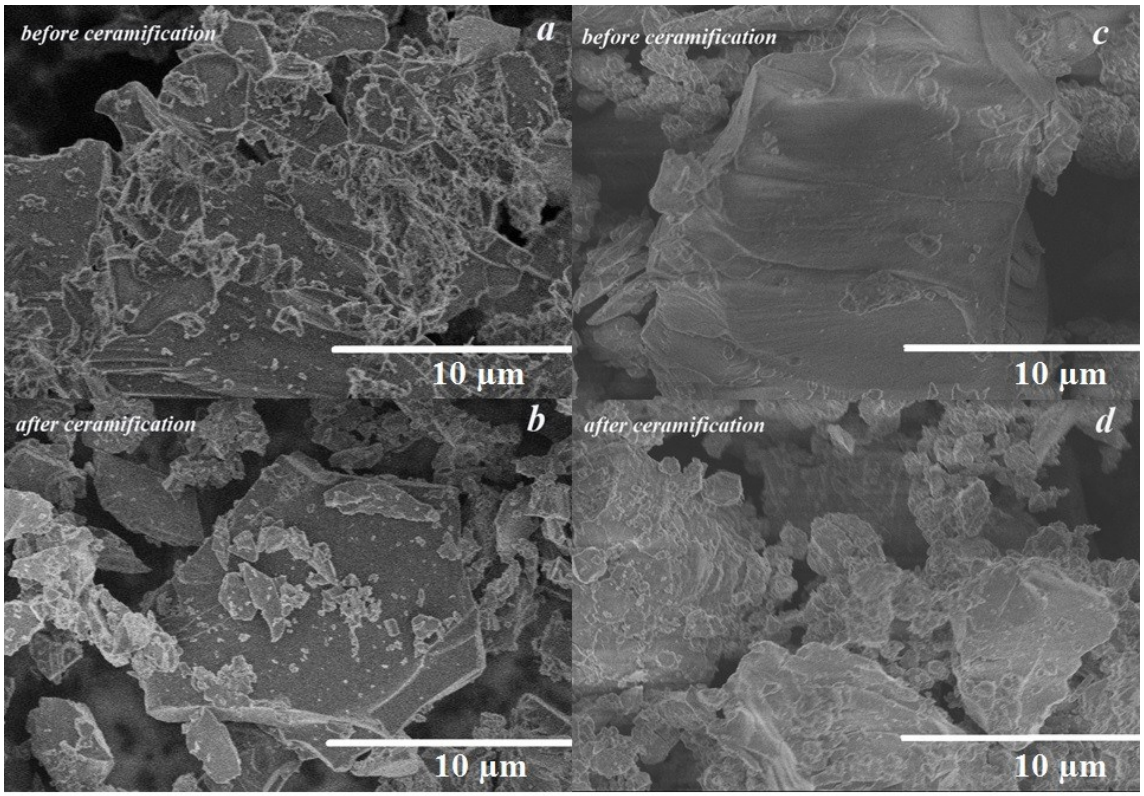

Fig. S3. a) SEM images of the TTCS cross-linked precursor before ceramification and **b)** TTCS pyrolysed powder obtained at 1273K. **c)** SEM images of the CERASET cross-linked precursor before ceramification and **d)** CERASET pyrolysed powder obtained at 1273K.

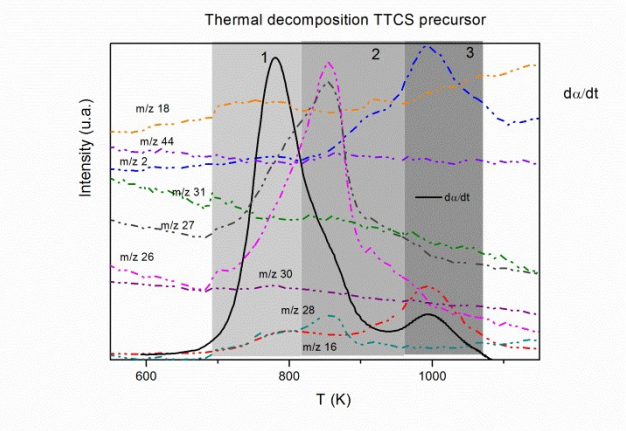

Fig. S4 Experimental Kinetic curves (dα/dt-T and signals m/z) obtained for the thermal decomposition of TTCS under Ar gas flow and linear heating rate 2 K $min^{-1}$and registered flow gas in spectrometer mass during the thermal decomposition

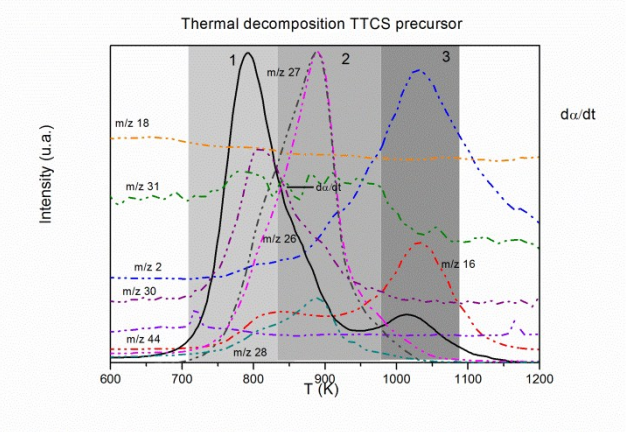

Fig. S5 Experimental Kinetic curves (dα/dt-T and signals m/z) obtained for the thermal decomposition of TTCS under Ar gas flow and linear heating rate 7.5 K $min^{-1}$and registered flow gas in spectrometer mass during the thermal decomposition

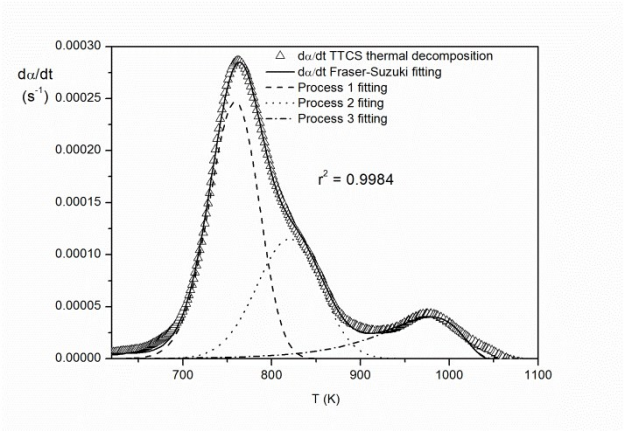

Fig. S6a Experimental kinetic curve (symbols) obtained for the thermal decomposition of TTCS at linear heating rate 2 K min^{-1} and the Fraser-Suzuki function (solid line) used for fitting the simulated curves. Three independent stages are plotted with dotted lines. Correlation coefficient has been included into the figure.

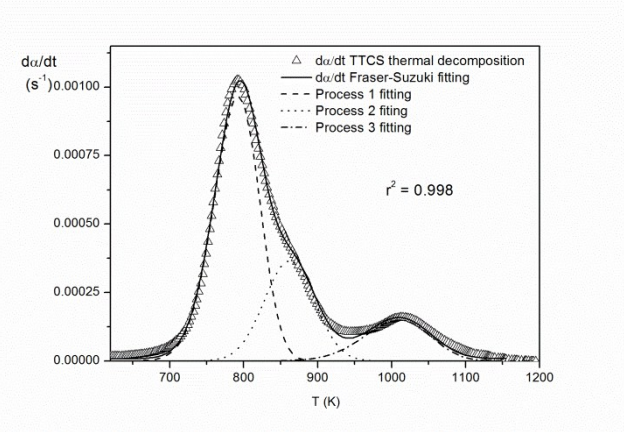

Fig. S6b. Experimental kinetic curve (symbols) obtained for the thermal decomposition of TTCS at linear heating rate 7.5 K min^{-1} and the Fraser-Suzuki function (solid line) used for fitting the simulated curves. Three independent stages are plotted with dotted lines. Correlation coefficient has been included into the figure.

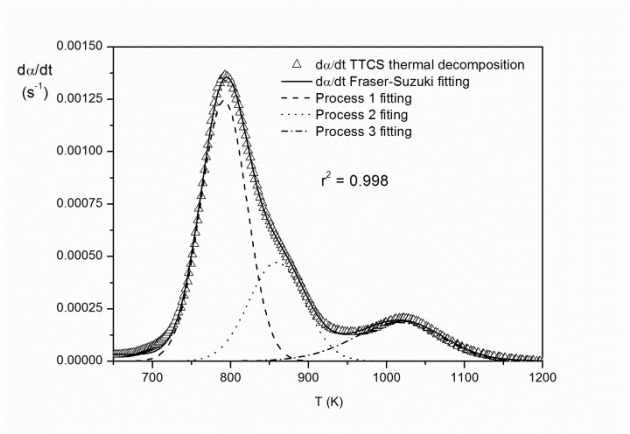

Fig. S6c. Experimental kinetic curve (symbols) obtained for the thermal decomposition of TTCS at linear heating rate 10 K min^{-1} and the Fraser-Suzuki function (solid line) used for fitting the simulated curves. Three independent stages are plotted with dotted lines. Correlation coefficient has been included into the figure.

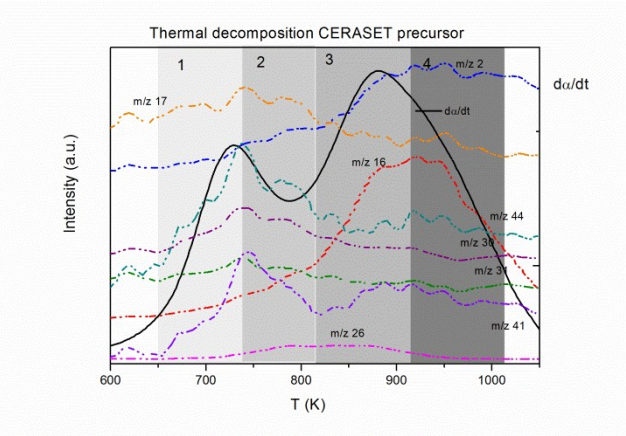

Fig. S7. Experimental Kinetic curves (dα/dt-T and signals m/z) obtained for the thermal decomposition of CERASET under Ar gas flow and linear heating rate 2 K $min^{-1}$and registered flow gas in spectrometer mass during the thermal decomposition.

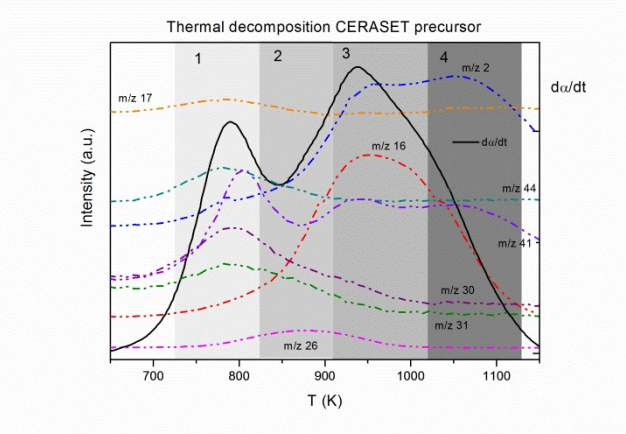

Fig. S8. Experimental Kinetic curves (dα/dt-T and signals m/z) obtained for the thermal decomposition of CERASET under Ar gas flow and linear heating rate 10 K $min^{-1}$and registered flow gas in spectrometer mass during the thermal decomposition.

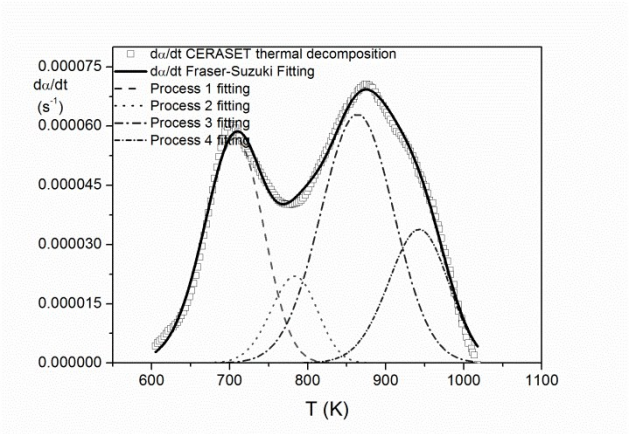

F **Fig. S9a.** Experimental kinetic curve (symbols) obtained for the thermal decomposition of CERASET at linear heating rate 1 K min^{-1} and the Fraser-Suzuki function (solid line) used for fitting the simulated curves. Four independent stages are plotted with dotted lines. Correlation coefficient has been included into the figure.

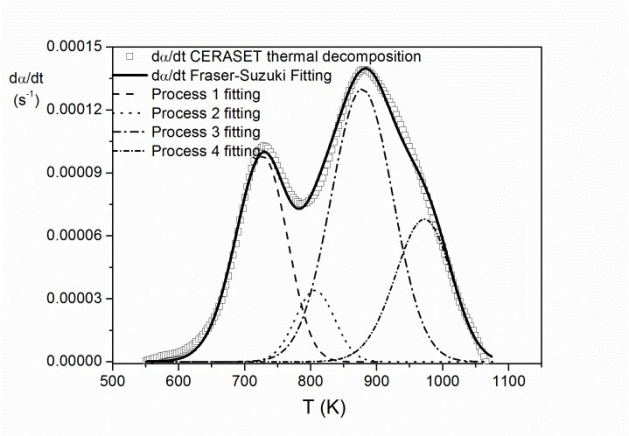

Fig. S9b. Experimental kinetic curve (symbols) obtained for the thermal decomposition of CERASET at linear heating rate 2 K min^{-1} and the Fraser-Suzuki function (solid line) used for fitting the simulated curves. Four independent stages are plotted with dotted lines. Correlation coefficient has been included into the figure.

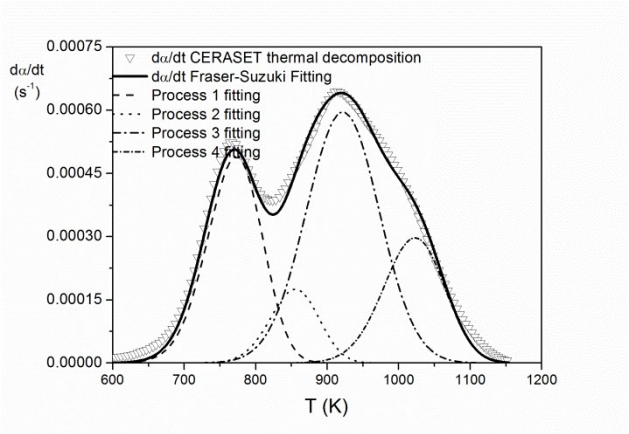

Fig. S9c. Experimental kinetic curve (symbols) obtained for the thermal decomposition of CERASET at linear heating rate 10 K min^{-1} and the Fraser-Suzuki function (solid line) used for fitting the simulated curves. Four independent stages are plotted with dotted lines. Correlation coefficient has been included into the figure.